

Figure 11: As in Figure 1 except for; (a) Exp DM, (b) Exp B1, and (c) Exp B3.

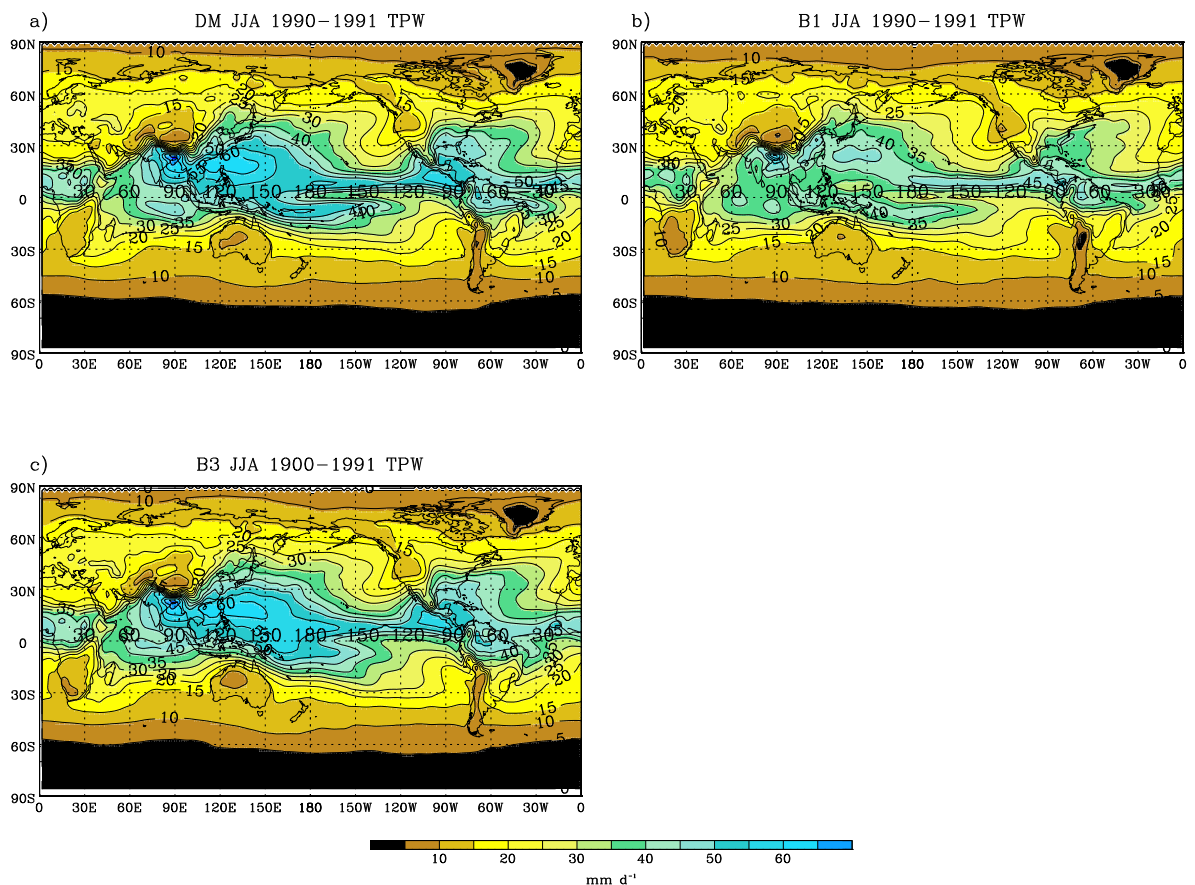


Figure 12: As in Figure 1 except for; (a) Exp DM, (b) Exp B1, and (c) Exp B3.

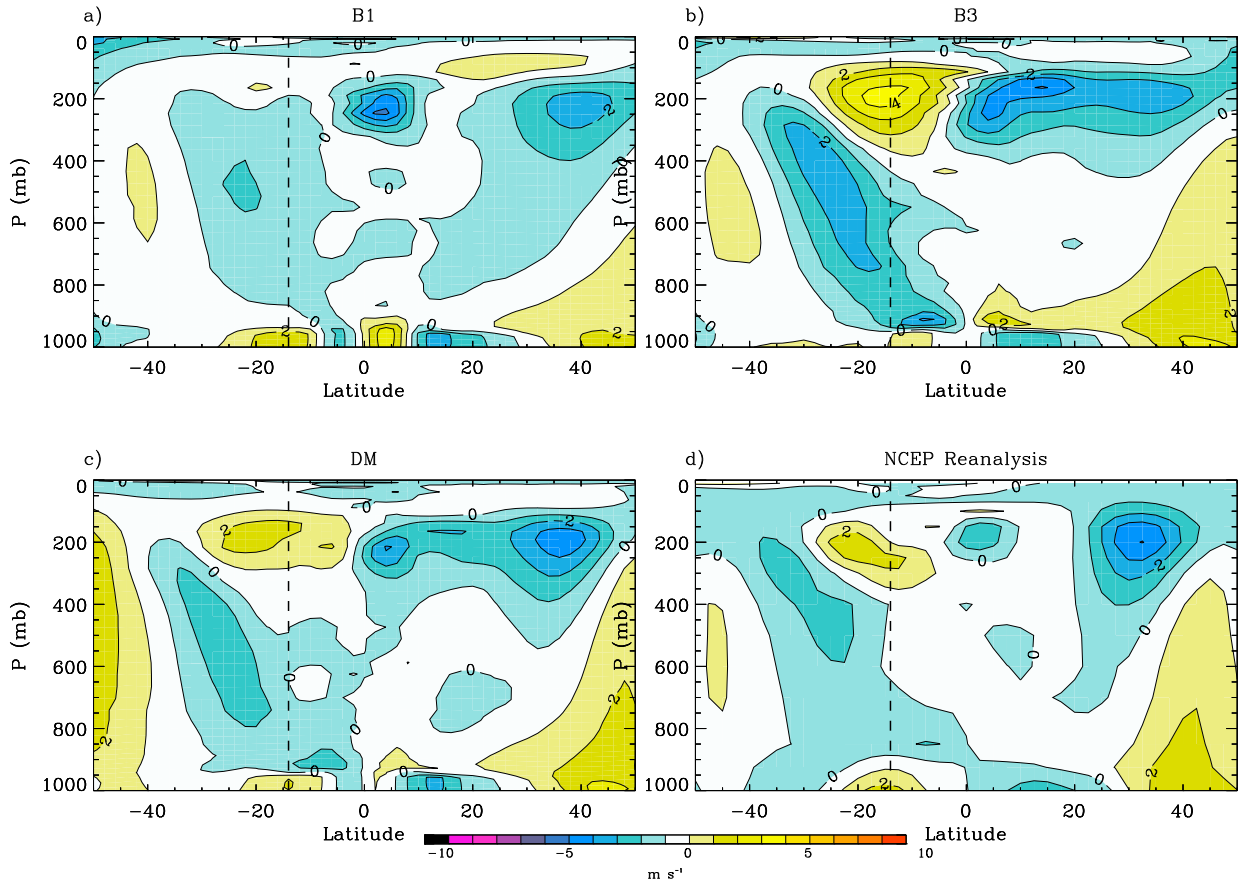


Figure 13: Meridional wind  $v$ , averaged between  $170^{\circ}\text{E}$  and  $150^{\circ}\text{W}$ , as a function of latitude and pressure, for JJA 1990-91: (a) Exp B1, (b) Exp B3, (c) Exp DM, and (d) NCEP re-analysis. The vertical dashed line indicates  $14^{\circ}\text{S}$  the southern edge of Box S.

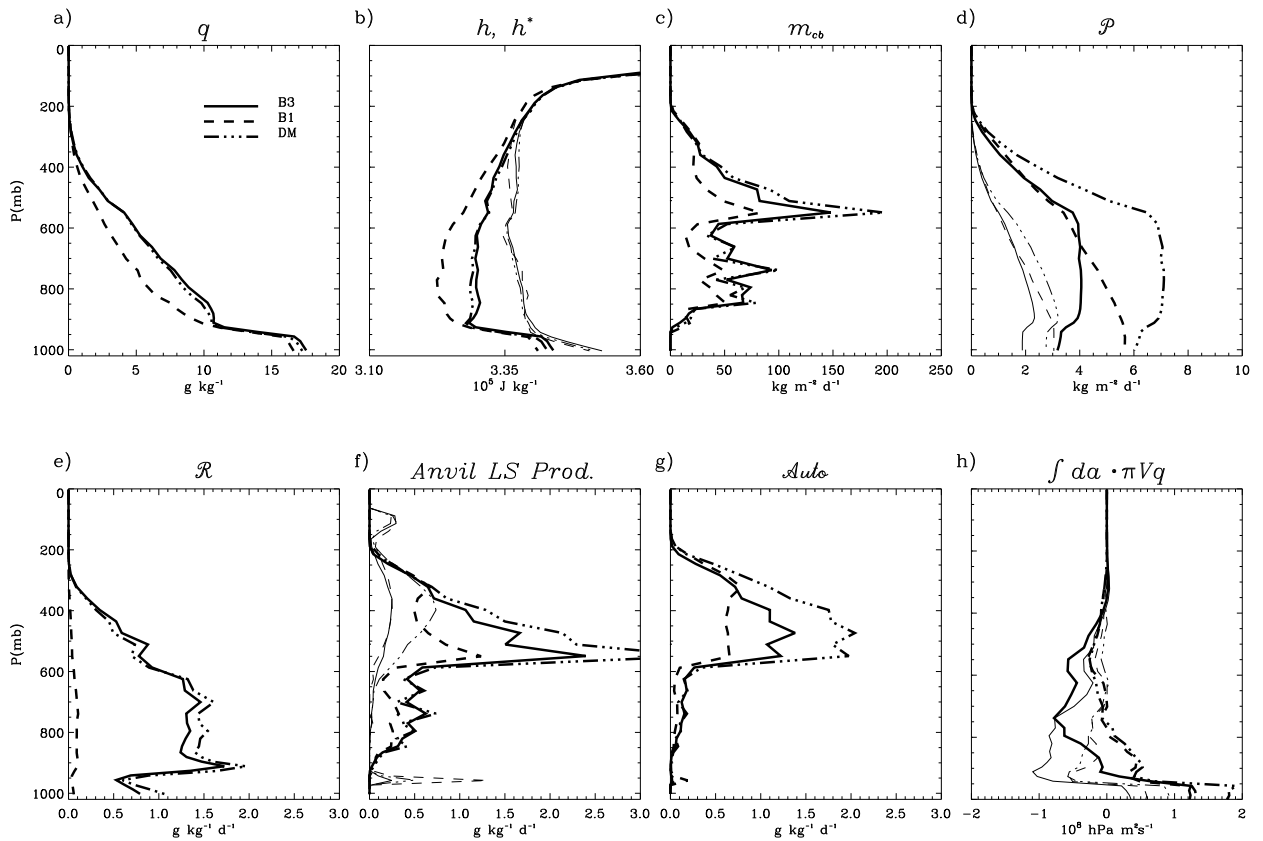


Figure 14: Box averaged profiles (for Box S) of various quantities from Exps B1, B3, and DM of: (a) specific humidity in  $\text{g kg}^{-1}$ ; (b) moist static energy  $h$  (thick lines), and saturated moist static energy  $h^*$  in  $\text{J kg}^{-1}$ ; (c) cloud-base convective mass flux  $m_{cb}$ , as a function of cloud detrainment pressure level, in  $\text{kg m}^{-2} \text{ d}^{-1}$ ; (d) precipitation flux  $\mathcal{P}$  in  $\text{kg m}^{-2} \text{ d}^{-1}$  (equivalent to  $\text{mm d}^{-1}$  at the surface); (e) moistening due to re-evaporation of rain in  $\text{g kg}^{-1} \text{ d}^{-1}$ ; (f) production of cloud condensate by detraining convection (thick lines) and RH-based, statistical condensation (thin lines) in  $\text{g kg}^{-1} \text{ d}^{-1}$ ; (g) autoconversion of cloud condensate to precipitation (large-scale only) in  $\text{g kg}^{-1} \text{ d}^{-1}$ ; and (h) net advective water vapor flux into Box S (thick lines) and net meridional flux (thin lines). In all panels, the solid line shows Exp B3, the dashed line shows Exp B1, and the dot-dashed line shows Exp DM.

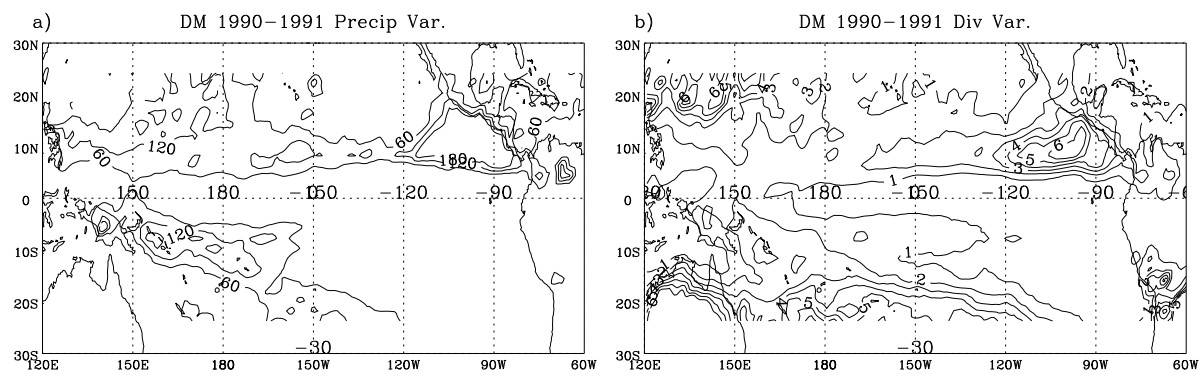


Figure 15: As Figure 3 for Exp DM: (a) precipitation variance; (b) variance of integrated PBL convergence.

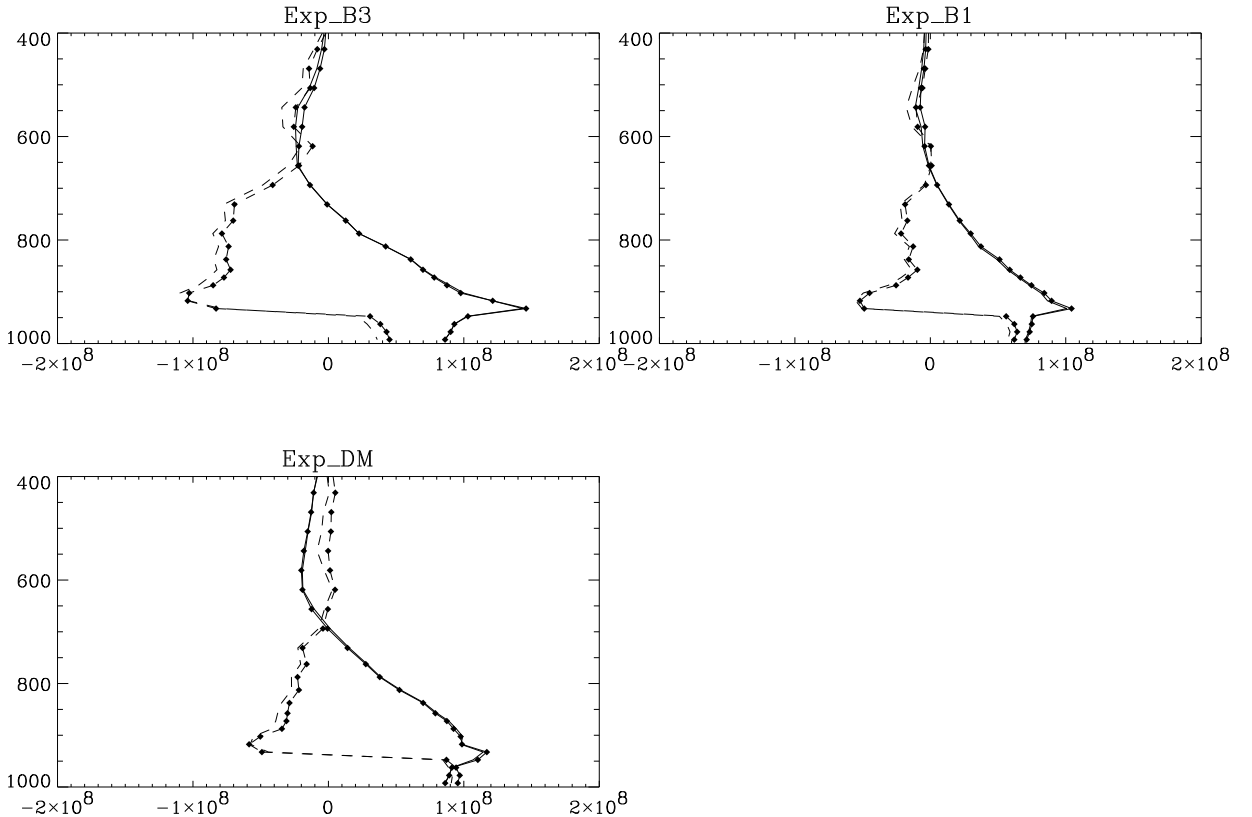


Figure 16: Profiles of horizontal water vapor fluxes ( $\text{hPa m}^2 \text{ s}^{-1}$ ) for JJA 1990 in Box S as functions of pressure (hPa): (top-left) Exp B3; (top-right) Exp B1; and (bottom-left) Exp DM. Thin solid lines with and without diamonds show net zonal flux, i.e.,  $\overline{\pi u q}^{\phi^S}_{\text{west}} - \overline{\pi u q}^{\phi^S}_{\text{east}}$ . Dashed lines with and without diamonds show net meridional fluxes  $\overline{\pi v q}^{\lambda^S}_{\text{south}} - \overline{\pi v q}^{\lambda^S}_{\text{north}}$ . Diamonds indicate that the fluxes shown are calculated from monthly-mean  $u$ ,  $v$ , and  $q$  fields. Profiles without diamonds indicate fluxes calculated from daily-average model fields.

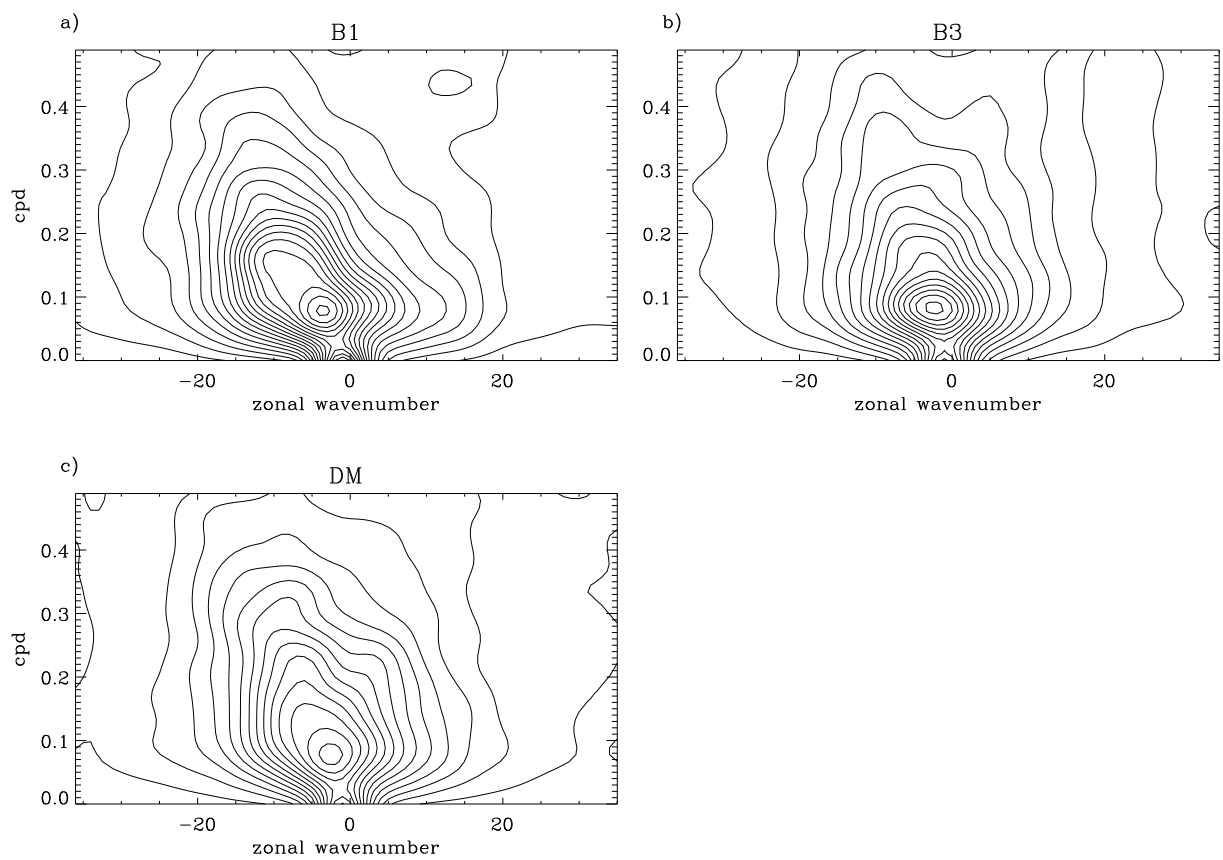


Figure 17: Space-Time (x-t) FFTs of precipitation along  $8^{\circ}\text{N}$  for daily data 1990-1991. Derived from 31-day high-pass filtered data.

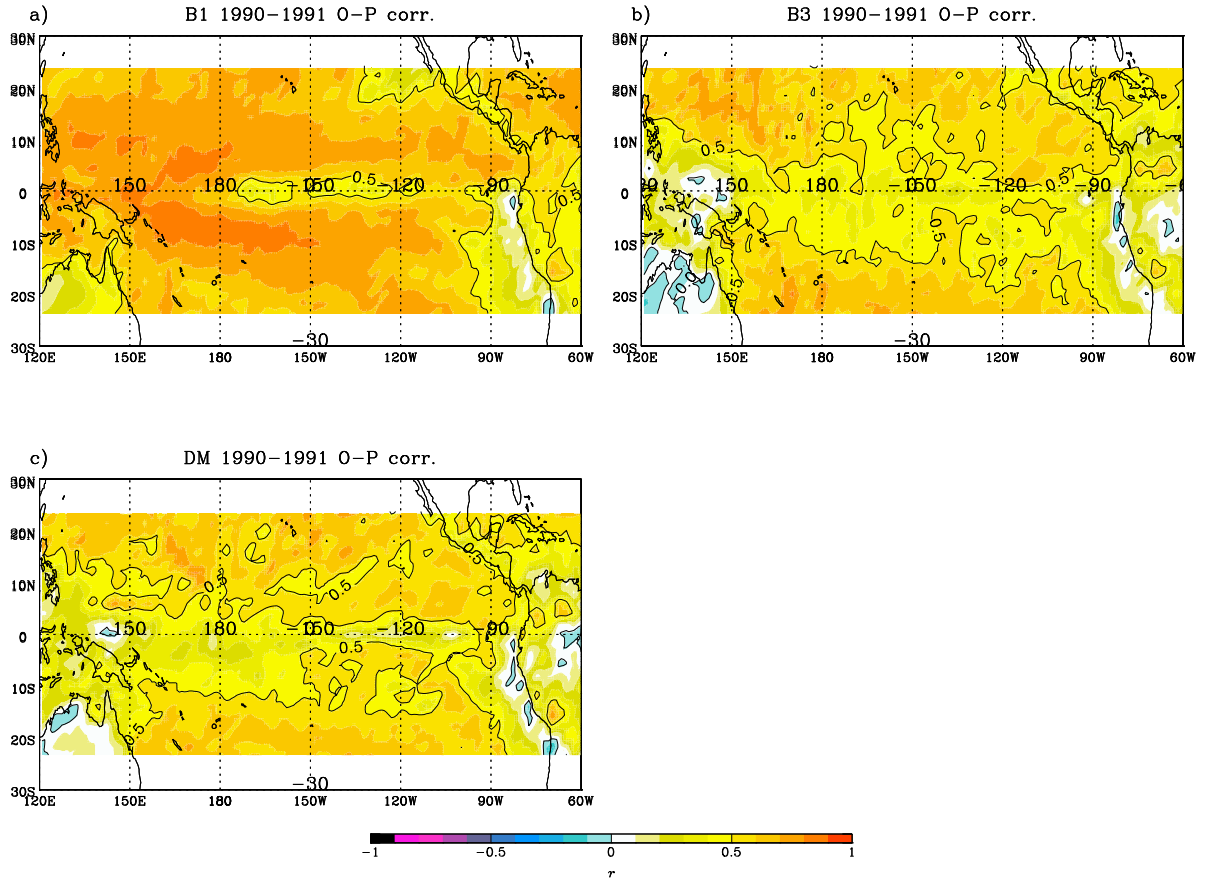


Figure 18: Time correlation of daily precipitation with integrated boundary layer convergence ( $\approx -\omega_{850}$ ) as a function of latitude and longitude, for 1990–1991. Derived from 31-day high-pass filtered data: (a) Exp B1; (b) Exp B3; and (c) Exp DM.

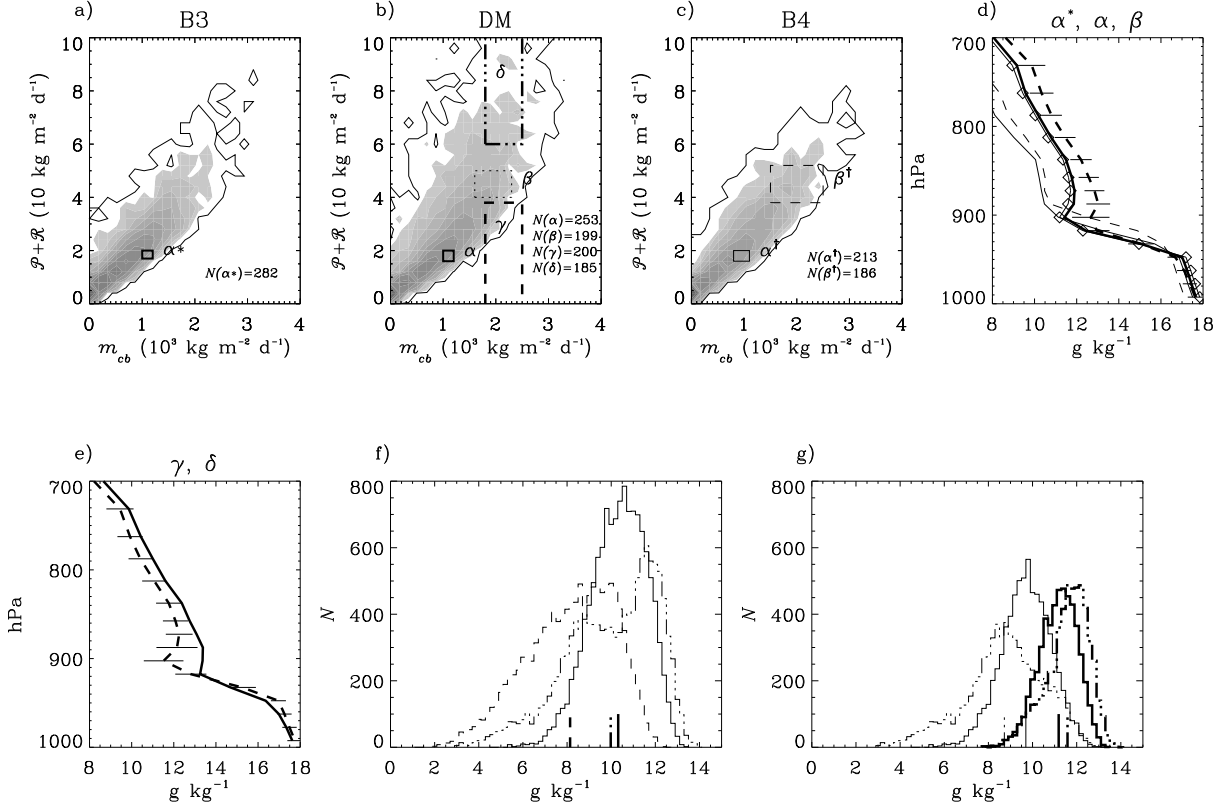


Figure 19: (a-c) Joint probability density functions (PDFs) for daily  $\mathcal{P}_g$  (vertical axis) and  $\sum_{<500} m_{cb}$  (horizontal axis), for June 1, 1990-Aug. 31 1990, for each gridpoint in Box S; a) Exp B3, b) Exp DM, and c) Exp B4. Daily average model results for 92 days at the  $8 \times 17$  gridpoints in Box S are used in the calculation of the PDFs. Results are binned into bins of  $0.173 \times 10^3 \text{ kg m}^{-2} \text{ d}^{-1}$  in the horizontal, and  $4 \text{ kg m}^{-2} \text{ d}^{-1}$  in the vertical. Thin contour indicates one occurrence out of a possible  $8 \times 17 \times 92 = 12,512$ . Successively darker shades indicate 2,4,8,16,32 ... occurrences. The rectangular areas in (a-c) labeled  $\alpha^*$ ,  $\alpha$ ,  $\beta$ ,  $\alpha^\dagger$ ,  $\beta^\dagger$ ,  $\gamma$ , and  $\delta$  contain populations of approximately equal size, which are used to form composite  $q$  profiles shown in (d-e). (d) Thick solid line shows composite  $q$ -profile for  $\alpha$ ; thick dashed line,  $\beta$ ; thin line with diamonds,  $\alpha^*$ ; thin solid line,  $\alpha^\dagger$ ; and thin dashed line,  $\beta^\dagger$ . The composites for  $\alpha^*$  and  $\alpha$  are nearly identical. Thin horizontal bars indicate  $1-\sigma$  for the  $\beta$  composite. Other populations have comparable spread. (e) Thick dashed line, profile for  $\gamma$ ; and thick solid line  $\delta$ . (f) PDFs of daily  $q$ , averaged between 800 and 900 hPa ( $\langle q \rangle_{800-900}^*$ ), in Box S for Exp B3 (solid) B1 (dashed) and DM (dot-dashed). (g) PDFs of daily  $\langle q \rangle_{800-900}^*$  sorted into convecting (thick lines) and “quiescent” (thin lines) sub-populations (see text). Dot-dashed lines in (g) indicate PDFs for DM and solid lines B3.